

Assessing Coulomb Collision Contributions to Photoelectron Deceleration above Earth's Polar Caps

Glyn A. Collinson^{1,2†}, Alex Glocer^{1†}, George Khazanov¹, Laila Andersson³, Suzie Imber⁴, Aroh Barjatya⁵, Rachel Conway⁵, James Clemmons⁶, Diana Swanson⁶, and Lance Davis⁶

¹Heliophysics Science Division, NASA Goddard Space Flight Center, Greenbelt, MD, USA

²G & K Rocket Yards, Interplanetary Expeditions, Criccieth, Gwynedd, UK

³Laboratory for Space and Atmospheric Physics, University of Colorado, Boulder, CO, USA

⁴Department of Physics and Astronomy, University of Leicester, Leicester, UK

⁵Space and Atmospheric Instrumentation Laboratory, Embry-Riddle Aeronautical University, Daytona Beach, FL, USA

⁶College of Engineering and Physical Sciences, University of New Hampshire, Durham, NH, USA

*

Key Points:

- We report the first measurement of coulomb collisions slowing photoelectrons escaping from Earth's atmosphere.
- This effect was previously masked by a spacecraft wake disturbance during the transition from supersonic to subsonic plasma wave speeds.
- Fully kinetic models are needed for precision studies of coulomb collision effects as existing analytical models overestimate energy shifts.

*†- Glyn Collinson and Alex Glocer contributed equally to this study

Corresponding author: G. Collinson, glyn.collinson@nasa.gov

Abstract

NASA’s *Endurance* rocket mission resolved a subtle energy shift in photoelectrons escaping from Earth’s polar caps, from which the first successful measurement of Earth’s ambipolar electrostatic field was made. Preflight models predicted that coulomb collisions with thermal electrons could add an extra energy shift of up to 1 eV. However, no such additional shift was reported in the initial analysis. Here, we identify a previously unreported effect related to the spacecraft wake, which introduced a systematic $+0.25eV$ energy shift that countered and masked the shift from coulomb collisions. After applying an in-flight calibration for this wake effect, we find a total photopeak energy shift consistent with the combined influence of the ambipolar field and the subtler $-0.37eV$ coulomb shift, predicted by the fully kinetic STET model. Further analysis of these recalibrated measurements yields an ambipolar field estimate in close agreement with the initial analysis.

Plain Language Summary

When solar extreme ultraviolet (EUV) radiation strikes neutral atoms in the atmosphere high-energy photoelectrons are released that can escape Earth’s gravity. NASA’s *Endurance* mission, with its high-resolution Photoelectron Spectrometer (PES), resolved a subtle energy shift in these photoelectrons as they escaped from Earth. Initial PES data analysis found that the energy shift was entirely consistent with Earth’s global ambipolar electrostatic field. However, preflight models also predicted that coulomb collisions (elastic collisions between photoelectrons and lower-energy thermal electrons), would create an additional shift ontop of that from the ambipolar field. However, no evidence for this additional shift was reported. In this study, we find that a previously unknown spacecraft effect canceled and masked this coulomb collisional effect. We also show that preflight models substantially overestimated this effect. After in-flight calibration, the measured shift matched predictions from the combined ambipolar field and a weaker coulomb shift, as estimated by the fully kinetic STET model.

1 Introduction: Photoelectrons and Coulomb Collisions

Electrons in Earth’s ionosphere consist broadly of two populations. They are dominated ($> 99.9\%$) by a thermal (or “core”) population ($< 1eV$), which is restrained from escaping from Earth by a global “ambipolar” electrostatic field (G. A. Collinson et al., 2024). Additionally, there exists a hot suprathermal population ($1eV$ to $\sim 100eV$), primarily generated between 130km-300km (depending on solar zenith angle) by photoelectron emission from the neutral atmosphere as a result of solar EUV radiation (Doering et al., 1976; Peterson et al., 1977; G. A. Collinson, Glocer, Pfaff, et al., 2022). Photoelectrons have more than enough energy to overcome gravity and escape to space, and have been observed at large distances down the magnetotail (Coates et al., 1985).

The energy spectrum of photoelectrons from any planetary atmosphere exhibits numerous discrete spikes (called “photopeaks”) (Lee et al., 1978, 1980a, 1980b; Jasperse & Smith, 1978). This is a result of the intense solar He-II emission line at 30.4nm which bombards the neutral gas with an excess of photons at one discrete energy. Consequently, photoelectrons are ejected at a range of discrete peaks, the energy of which is that of the photon ($40.78eV$) minus the work function of the specific electron orbital from which they escaped. The result is that planetary ionospheres radiate electrons at discrete and known energies, rigidly dictated by atomic physics. As a result, He-II photopeaks have been used throughout the solar system as tracers of parallel electrical potentials (Coates et al., 1985, 2015; G. Collinson et al., 2015; G. A. Collinson et al., 2016, 2023; Xu et al., 2018). If the photopeaks are observed at a different energy from which they are known to have been created, it is usually assumed this is primarily due to their falling from an electric potential drop between their source in the atmosphere and the spacecraft.

71 However, in theory photoelectrons should receive an additional retardation from coulomb
 72 collisions with the thermal electron population (Spitzer, 1950; Cicerone & Bowhill, 1970;
 73 Swartz et al., 1971; Khazanov et al., 1997). As photoelectrons corkscrew upwards along
 74 magnetic field lines, they are predicted to scatter elastically with the cold thermal elec-
 75 trons, transferring (and losing) some of their energy. As a result, one expects to observe
 76 an additional decrease in photoelectron energy with increasing altitude from coulomb
 77 collisions.

78 While coulomb collisions in general are a well-established phenomenon, to our knowl-
 79 edge, this net slowing effect on Photoelectrons has never been successfully resolved ob-
 80 served experimentally. This is because until recently, no electron spectrometer has ex-
 81 isted with sufficient resolution to fully resolve the He-II photopeaks, let alone the sub-
 82 tle slowing by the coulomb collisions with the thermal core electron population. The clos-
 83 est to date was *Atmospheric Explorer E*, which measured photopeaks to $1.5\%\Delta E/E$. Anal-
 84 ysis of AE-E data by Lee et al. (1980b) found an order of magnitude agreement between
 85 the observed energy loss due to coulomb collisional scattering and theory, which was deemed
 86 satisfactory given the large number of assumptions necessary in their calculations. Fur-
 87 thermore, Lee et al. (1980b) were not able to separate out the effect of the ambipolar
 88 field in their calculations.

89 NASA’s *Endurance* sounding rocket (yard №47.001) (G. A. Collinson, Glocer, Pfaff, et
 90 al., 2022) launched May 11th 2022 to an altitude of 768km, carrying the new Photoelec-
 91 tron Spectrometer (PES) instrument, with an unprecedented energy resolution of $0.5\%\Delta E/E$.
 92 PES successfully resolved one of the brightest He-II photopeaks throughout the major-
 93 ity of its 15 minute suborbital flight. PES measured an energy shift of this photopeak
 94 of $-0.55 \pm 0.09eV$ between the photoproduction region (250km) and apogee, exactly
 95 what was expected from the ambipolar field of Earth under the specific conditions of the
 96 flight (G. A. Collinson et al., 2024).

97 No clear evidence was reported of an additional photopeak energy shift from coulomb
 98 collisions. This was in contrast to preflight predictions using the GLOW two stream mode
 99 (Solomon, 2017), which suggested as much as $\sim -1eV$ of additional energy decrease could
 100 be seen from coulomb collisions alone (G. A. Collinson, Glocer, Pfaff, et al., 2022). As
 101 per Solomon (2017) GLOW models the shift associated with coulomb collisions using the
 102 analytical formulation by Swartz et al. (1971), which does not take into account key phys-
 103 ical effects such as pitch-angle scattering. Given that such an additional $\sim -1eV$ shift
 104 would have been readily observable to PES, it was concluded that the formulation by
 105 Swartz et al. (1971) must be substantially overestimating the effect. The close agreement
 106 between the observed photopeak shift and that predicted for an ambipolar field suggested
 107 that the slowing effect by coulomb collisions must in reality be more subtle. G. A. Collinson
 108 et al. (2024) thus used a simple linear trend in their calculations to not risk not over-
 109 fitting the PES data, and assumed that any photoelectron deceleration by coulomb col-
 110 lisions must in reality be small and within the uncertainty of the measurement

111 In this paper, we examine fine details of the structure of the observed shift in photoelec-
 112 trons measured by the *Endurance* PES instrument, searching for evidence of the addi-
 113 tional energy decrease expected from coulomb collisions. We use the fully kinetic Superther-
 114 mal Electron Transport (STET) model (Khazanov et al., 2014) to self-consistently model
 115 the additional shift from coulomb collisions, finding it to be far smaller ($-0.37eV$ at apogee)
 116 than predicted by the Swartz et al. (1971) analytical model used in GLOW.

117 This paper is organized as follows. In section 2, we give a brief summary of the *Endurance*
 118 mission and the instruments used in this study. In section 3, we closely examine the ver-
 119 tical structure of the shift in photoelectrons, finding the need for an additional in-flight
 120 calibration for a hitherto unknown observational effect which provided a systematic (and
 121 unphysical) $+0.25eV$ increase in photoelectron energy between 550 km and 620 km. In
 122 section 4, we perform an additional in-flight calibration and compare the observed en-

123 ergy decrease against that expected from two effects: ambipolar field (predicted from in-
 124 situ data from another instrument) and coulomb collisions (from the fully kinetic STET
 125 model). In section 5, we summarize our findings and present our conclusions.

126 **2 NASA Rocketship 47.001 *Endurance***

127 In this section we give a brief summary of the *Endurance* rocket mission and the instru-
 128 ments relevant to this study. For a detailed description of the mission design and the PES
 129 instrument see G. A. Collinson, Glocer, Pfaff, et al. (2022). For a summary of the main
 130 results see G. A. Collinson et al. (2024).

131 **2.1 Mission Overview**

132 The *Endurance* rocketship launched at 01:31 GMT on May 11th 2022 from Ny Ålesund,
 133 Svalbard. The entire flight occurred on open magnetic field lines in Earth’s north po-
 134 lar cap. *Endurance* was a three axis stabilized spacecraft, aligned with Earth’s magnetic
 135 field to within 3.5° degrees.

136 Figure 1a shows a time versus altitude plot of the mission. The color coded timeline above
 137 gives a summary of the main events. The primary mission was divided between 70 s of
 138 uninterrupted science collection (blue, Fig. 1a), followed by 10 s where the attitude con-
 139 trol system was free to fire and realign the rocketship with Earth’s magnetic field (yel-
 140 low, Fig. 1a). The cold gas produced by these firings interfered with every instrument
 141 apart from the camera. However, all the gas rapidly dispersed before commencement of
 142 the next science collection, and did not contaminate science measurements.

143 Just after apogee (768km), *Endurance* performed a pitch over maneuver (green, Fig. 1a),
 144 rotating by 180° so that the instruments on the bow of the rocketship would look into
 145 the ram direction on the downleg portion of the flight.

146 **2.2 *Endurance* instruments used for this study**

147 The primary instrument used in this paper is the photoelectron spectrometer (PES), a
 148 new technology developed for the mission (G. A. Collinson et al., 2018; G. A. Collinson,
 149 Glocer, Chornay, et al., 2022). PES simultaneously measured two data products every
 150 10s. A standard energy resolution ($15\%\Delta E/E$) survey between 10eV and 1keV, and a
 151 high resolution ($0.5\%\Delta E/E$) scan between 20.3eV and 25.85eV to attempt to resolve
 152 the most prominent He-II photopeaks, of which it successfully caught one, dominated
 153 by the $N_2A^2\Pi_u$ atomic transition. PES was a pure energy spectrometer, with two fixed
 154 look directions, field aligned and anti-aligned. In this paper we only use the high res-
 155 olution measurements of photoelectrons escaping from Earth’s ionosphere (i.e. aft-facing
 156 during upleg and prior to pitch-over, bow-facing after pitch-over to loss of signal).

157 This study also uses data from the *Endurance* Swept Langmuir Probe (SLP). This is a
 158 traditional needle probe mounted at the very bow of the spacecraft. A voltage sweep was
 159 applied once every 5 seconds during the flight, and the current measured by the probe
 160 recorded. From this, we may determine the density and temperature of ionospheric ther-
 161 mal electrons ($< 1eV$). These two parameters can be combined to calculate electron pres-
 162 sure, and hence predict the strength of Earth’s ambipolar electric field according to equa-
 163 tion 1.

$$E_{||} = \frac{\nabla P_E}{n_e q} \quad (1)$$

164 SLP also measured the electrical potential difference between the spacecraft and the am-
 165 bient plasma. This spacecraft vs. plasma potential is crucial to calibrate PES, since pho-

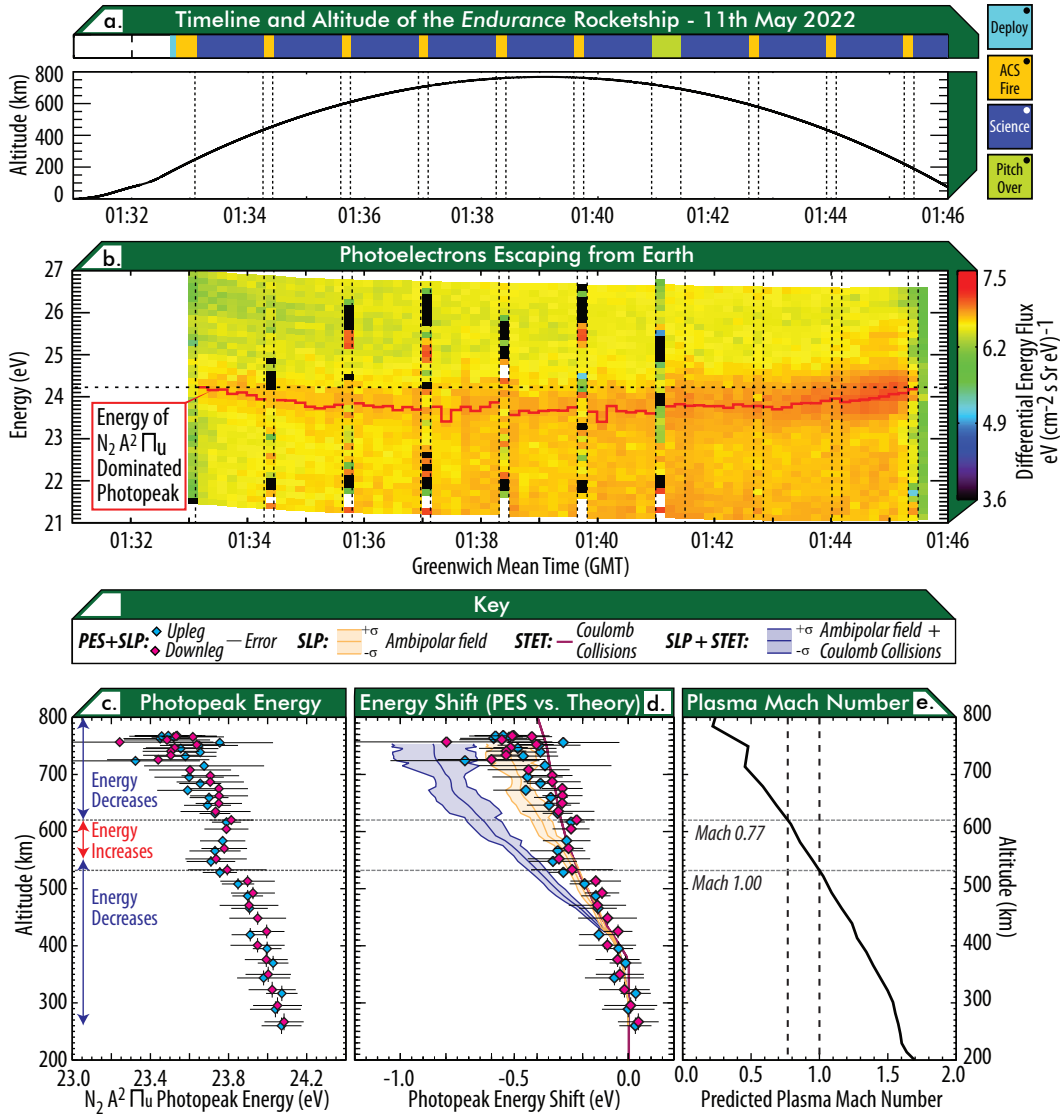


Figure 1. a.) Color coded timeline of the *Endurance* mission and plot of time vs. altitude of the rocketship. b.) High-resolution spectrogram showing the evolution of differential flux of the primary He-II photopeak during the flight, corrected for spacecraft potential. c.) Energy vs. Altitude of the primary He-II photopeak, corrected for spacecraft potential. d.) Comparison between the energy shift of the He-II photopeak and i.) the predicted shift from the ambipolar field from SLP (gold), ii.) the energy shift from coulomb collisions alone from the STET model (maroon), and the combined shift from both effects (purple). e.) Calculation of the evolution of Plasma Mach number with altitude according to Gombosi and Rasmussen (1991).

166 photoelectrons escaping from the ionosphere fall through two potential drops: Earth’s elec-
 167 trical potential, and the spacecraft potential. It is crucial to remove the spacecraft ef-
 168 fects in order to accurately measure Earth’s ambipolar field and to search for the sub-
 169 tle energy shift of the photopeaks due to coulomb collisions. All PES data shown in this
 170 study have been corrected for spacecraft potential by SLP.

171 **3 Analysis of the altitude structure of the He-II Photopeak**

172 Figure 1b shows a time vs. energy spectrogram of PES high-resolution measurements
 173 of outflowing photoelectrons. These data have been corrected for spacecraft potential
 174 as measured by SLP, as per G. A. Collinson et al. (2024). A bright He-II photopeak was
 175 observed throughout the flight, presumed to be dominated by the $N_2A^2\Pi_u$ transition
 176 at 24.09 eV. The peak energy of this photopeak was determined by fitting a gaussian dis-
 177 tribution to each scan. A general trend towards lower energies near apogee was observed
 178 over the flight. Figure 1c shows a plot of energy versus altitude of the peak energy from
 179 this gaussian fit, showing measurements on upleg (blue) and downleg (pink).

180 Figure 1d shows the magnitude of the shift in energy of the He-II photopeak from its
 181 production energy (24.09eV). The gold curve shows the predicted energy shift from the
 182 ambipolar field of Earth according to the SLP instrument, using equation 1. From this
 183 very close agreement, G. A. Collinson et al. (2024) concluded that the only source of the
 184 shift apparent in photoelectron energy was from the ambipolar field.

185 **3.1 Apparent initial non-detection of an additional energy shift from coulomb** 186 **collisions**

187 Pre-flight simulations using the GLOW two-stream model predicted that an additional
 188 shift of as much as 1eV would be present due to coulomb collisions (G. A. Collinson, Glo-
 189 cker, Pfaff, et al., 2022). However, GLOW does not self-consistently model this effect, and
 190 it predicts this additional shift from an analytical model (Swartz et al., 1971). Addition-
 191 ally, *Endurance* is the first mission to resolve photopeaks with sufficient resolution to em-
 192 pirically test this aspect of the model. The 1eV of additional shift predicted by GLOW
 193 would have been readily seen by PES. Thus the most likely explanation for this appar-
 194 ent non-detection is that the analytical model underpinning this calculation in GLOW
 195 is substantially overestimating the shift due to coulomb collisions.

196 For the purposes of G. A. Collinson et al. (2024), which was to calculate an average po-
 197 tential drop over the entire flight, it was assumed that any additional coulomb collisional
 198 shift must be far smaller than predicted by GLOW, and were being swallowed by the
 199 uncertainties in the measurement. We shall test this assumption in this paper.

200 For this study we used the fully kinetic Superthermal Electron Transport (STET) model
 201 (Khazanov et al., 2014) configured for an open field line as in Glocer et al. (2017) to more
 202 accurately predict the extra photopeak energy shift from coulomb collisions. We more-
 203 over configure the model to use the observed thermal electron density from the SLP and
 204 ran STET at a very high energy resolution to ensure a good fidelity result. The struc-
 205 ture of the thermosphere for the model was in good agreement with that measured by
 206 the *Endurance* Bayard-Alpart Ionization Gauge (G. A. Collinson, Glocer, Pfaff, et al.,
 207 2022). STET self-consistently calculates the gyroaveraged electron distribution function
 208 as a function of energy, pitch angle, and position along the field line. This calculation
 209 includes production and transport of photoelectrons along a magnetic field line, and ex-
 210 plicitly calculates coulomb collisions (Khazanov et al., 2014). Details of the collisional
 211 operator used in STET are provided in Khazanov (2010). STET predicts a total shift
 212 of $-0.37eV$ at apogee from coulomb collisions alone (Fig. 1d, maroon line).

213 The purple curve in Fig. 1d takes the ambipolar field calculation from the SLP instru-
 214 ment and adds to it the additional coulomb energy shift predicted by STET. We note
 215 the following features of this prediction. Between 250km and 380km, no additional shift
 216 from coulomb collisions is predicted. This is because photoelectrons are still being pro-
 217 duced throughout these altitudes and thus the photopeaks are still at their energy of pho-
 218 toemission. Between 430km and ~ 600 km, the two curves (Fig. 1d gold vs. purple) slowly
 219 diverge due to an additional energy shift from coulomb collisions. Above ~ 600 km, the
 220 gradient of the two curves approximately match. This is because by these altitudes *En-*
 221 *durance* had flown out of the bulk of the ionosphere and coulomb collisions are so infre-
 222 quent that the energy shift is dominated by the ambipolar field.

223 **3.2 Investigation of an anomalous increase in photoelectron energy be-** 224 **tween 550km and 620km**

225 A closer analysis of the fine structure of the PES data is required before we may search
 226 for evidence of the effect of coulomb collisions. Between ~ 250 km and 550 km (upleg and
 227 downleg), the measured energy of the primary photopeak decreases in energy, a trend
 228 one would generally expect from either ambipolar field, coulomb collisions, or a combi-
 229 nation of both (purple, Fig. 1d). However, between 550 km and 620 km, this trend re-
 230 verses, with the photopeak unexpectedly increasing in energy (Fig. 1c). Given that this
 231 was observed on both upleg and downleg (separated by ~ 150 km downrange distance),
 232 it is extremely unlikely that this increase in energy is random, and is in all probability
 233 a real effect.

234 There is no known natural phenomenon which should cause an apparent energy increase
 235 of photoelectrons at these altitudes. The most plausible explanation is if there is an ad-
 236 ditional spacecraft effect (beyond spacecraft potential) which is altering the energy of
 237 photoelectrons as they approach the PES sensors. The data (Fig. 1c) suggest that what-
 238 ever this spacecraft effect is, was in a stable state below 550 km, in a different stable state
 239 above 620 km, and gradually transitioned in-between.

240 We posit that this effect is related to the plasma wake of *Endurance*, and in particular,
 241 how it changed between the transition from supersonic to subsonic flight. All spacecraft
 242 create a wake as they travel through the plasma (or as the plasma flows over them). The
 243 vast majority of spacecraft are supersonic with respect to the ambient plasma, gener-
 244 ating a shockwave around them just like a jet fighter or the Concorde supersonic trans-
 245 port. *Endurance* however was a ballistic sounding rocket, with velocity varying between
 246 3.0km/s at 250 km, and 0.4km/s near Apogee. We hypothesize that the increase in pho-
 247 topeak energy between 550 and 620 km is an effect arising from the transition between
 248 supersonic and subsonic flight, and a fundamental change in the nature of the plasma
 249 wake of the spacecraft.

250 If this theory is correct, the altitudes at which *Endurance* was transonic should match
 251 the altitudes at which the photoelectron shift occurred (550 km to 620 km). In other words,
 252 *Endurance* should be supersonic below ~ 550 km and subsonic above 620km.

253 To calculate the mach number (M) for the plasma wake of *Endurance*, we take the rocket
 254 velocity (V_r) and divide by the wave speed in the ambient plasma (a) at a given altitude,
 255 according to equation 2.

$$M = \frac{V_r}{a} \quad (2)$$

256 Where we take a from Gombosi and Rasmussen (1991), in the approximation neglect-
 257 ing heat flow as below in equation 3.

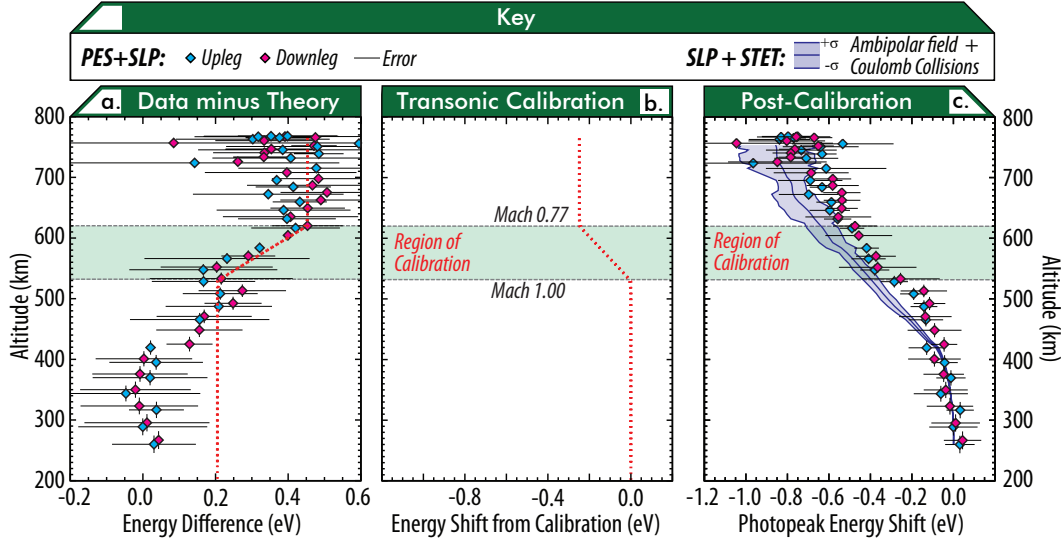


Figure 2. a.) Difference between the measured shift in photoelectrons by PES and predicted combined shift from ambipolar fields (from SLP) and coulomb collisions (from STET). b.) Transonic calibration factor vs. altitude. c.) Magnitude of the shift in the He-II photopeak vs. altitude, as Fig. 1d but with in-flight transonic calibration.

$$a = (3a_e^2 + 3a_i^2)^{0.5} \quad (3)$$

258 Where a_e and a_i are defined as below in equations 4 and 5.

$$a_e^2 = \frac{kT_{e||}}{m_i} \quad (4)$$

$$a_i^2 = \frac{kT_{i||}}{m_i} \quad (5)$$

259 Fig. 1e shows a plot of plasma Mach number versus altitude for the conditions encountered
 260 during the flight of *Endurance*. We used data from the EISCAT Svalbard Radar
 261 collected during the rocket flight in this calculation (see G. A. Collinson et al. (2024),
 262 extended Figure 6). Supersonic flight is predicted up to ~ 530 km, near the altitude at
 263 which photoelectrons begin to unexpectedly increase in energy. The altitude range up
 264 to 620 km corresponds to a transonic region where plasma Mach number drops down to
 265 Mach 0.77. Fig. 1e is this consistent with the hypothesis that this altitude range is as-
 266 sociated with a substantial change in the character of the plasma wake, and presumably
 267 collapse of the supersonic shockwave generated by the spacecraft.

268 4 Results

269 4.1 In-flight Transonic Calibration

270 Understanding the specific physics of how the transonic transition is affecting the ap-
 271 parent energy of the photopeaks, and why specifically this effect appears to stop below
 272 Mach 0.77, would require additional modeling, and is beyond the scope of this study (al-
 273 though we speculate briefly in Section 5). However since PES consistently measured this

274 effect on both upleg and downleg, we choose to calibrate it out of the PES data. One
 275 approach to measure the additional energy offset from this transonic effect would be to
 276 measure the total net increase in energy between 550km and 620km. However, this ne-
 277 glects the fact that what is being measured by PES in this altitude region is a combi-
 278 nation of an energy increase from the spacecraft wake and a presumed decrease from both
 279 ambipolar field and coulomb collisions. We thus chose the baseline of our calibration to
 280 be the predicted shift expected from these combined known effects.

281 Figure 2a shows the difference between the measured energy shift from PES (as in Fig.
 282 1d) and the combined energy shift expected from the ambipolar field (from SLP) and
 283 the coulomb collision shift (from STET). Below 420 km, PES observations align closely
 284 with theory, showing a near-zero energy difference. Above 620 km, there is a constant
 285 offset between the measured and predicted values. The energy difference between the-
 286 ory and observations remains constant, meaning the gradient of the PES measurements
 287 aligns with theoretical expectations. This suggests that, at higher altitudes where coulomb
 288 collisions are minimal, the observed PES energy shift from 620 km to apogee is largely
 289 governed by the ambipolar field, as predicted by theory.

290 Between 420 km and 620 km, the data gradually diverges from theoretical predictions.
 291 There could be numerous causes of this, not the least that STET is still over-estimating
 292 the effects of coulomb collisions. Applying a correction factor across this entire altitude
 293 range might risk overfitting, so we limit the in-flight calibration to altitudes between 530
 294 km and 620 km. This range begins at the predicted altitude where *Endurance* drops be-
 295 low Mach 1 (Fig. 1e) and spans the region where an unphysical increase in photoelec-
 296 tron energy was observed (Section 3.2).

297 Figure 2b presents the transonic in-flight calibration derived from this analysis. No cor-
 298 rection is applied below 530 km. Between 530 km and 620 km, the calibration factor in-
 299 creases linearly (fitted to Fig. 2a) to counter the erroneous energy shift from the space-
 300 craft wake. Above 620 km, only a constant offset of $-0.25eV$ is applied. We will now
 301 use this calibration factor to correct the PES data for the transonic wake effect.

302 4.2 Examination of the post-calibration energy shift with altitude of the 303 He-II photopeak

304 Figure 2c shows a plot of the evolution with altitude in the relative shift of the He-II pho-
 305 topeak after the transonic in-flight calibration (upleg in blue, downleg in pink). Data be-
 306 low 550km are identical to the shift in Fig. 2b. Data above 550 km have undergone the
 307 new in-flight calibration from the transonic energy shift correction (Fig. 2b). The total
 308 energy shift between 250 km and apogee is $-0.77 \pm 0.11eV$, greater than the $-0.55 \pm$
 309 $0.09eV$ reported by G. A. Collinson et al. (2024).

310 As in Fig. 1d, the purple curve in Fig. 2c shows the predicted combined shift from amb-
 311 ipolar field (from SLP measurements) and coulomb collisions (from STET). The newly
 312 re-calibrated PES data now agrees within errors of the combined predicted shift, con-
 313 sistent with a combination of both ambipolar field and coulomb collisions were deceler-
 314 ating the photoelectrons. A small systematic offset ($\sim 0.1eV$) is apparent in the data above
 315 450km. However, this is well within the measurement error of either the optics of the
 316 PES instrument, the spacecraft potential from SLP, or the coulomb collision shift esti-
 317 mation from STET.

318 5 Discussion and Conclusions

319 In this study we examined high resolution photoelectron spectra from NASA's *Endurance*
 320 sounding rocket. Our goal was to make the first measurement of the subtle additional
 321 energy decrease in the photoelectrons from coulomb collisions with the thermal (core)

322 electron population as they flow from their production region (250km-400km) to the near
 323 boundary of the magnetosphere (i.e. near Apogee at 768km). One of the key factors in
 324 the design of the mission was minimizing the effect of coulomb collisions. Pre-flight cal-
 325 culations using GLOW predicted that for high solar activity, the photopeaks may be com-
 326 pletely eroded by the time they reach apogee. Thus *Endurance* was deliberately flown
 327 near solar minimum, and during low solar activity. Thus the measurements presented
 328 here likely represent a case of minimal coulomb collisional effects. The PES instrument
 329 carried aboard *Endurance* is the first electron spectrometer with sufficient energy res-
 330 olution to be capable of observing this subtle effect. However, a previous analysis of PES
 331 data by G. A. Collinson et al. (2024) found the total shift in the photoelectrons to be
 332 entirely consistent with that expected only from Earth’s ambipolar electrostatic field,
 333 and reported no such additional shift from coulomb collisions.

334 **5.1 In-flight Transonic Calibration**

335 Before we could begin our search for the slowing of photoelectrons from coulomb colli-
 336 sions, we discovered an additional correction was required from a hitherto unreported
 337 spacecraft effect. Specifically, as the spacecraft slowed to subsonic speeds, the energy of
 338 photoelectrons was observed to unphysically increase by $+0.25eV$ between Mach 1 and
 339 Mach 0.77. This effect was observed again in reverse on the downleg as *Endurance* ac-
 340 celerated through the Transonic regime to supersonic flight. Further modeling is required
 341 to understand the detailed physics behind this additional energy shift associated with
 342 the Transonic transition. We posit one possibility is that the spacecraft wake could be
 343 causing a systematic offset in the measurement of spacecraft potential. Another expla-
 344 nation could be that the supersonic wake is physically slowing the photoelectrons (above
 345 Mach 1), possibly from an additional weak electric potential drop associated with the
 346 shockwave. Understanding the physics behind this effect, and why it dissipates around
 347 Mach 0.77 is a prime topic for future modeling studies. What is clear though is that the
 348 photopeak energy should not increase naturally over this altitude. Thus, for the purposes
 349 of this study we performed an in-flight calibration to remove this spacecraft effect. Note
 350 that data below 530km are untouched by this calibration, and data above 620km are only
 351 shifted by a constant $-0.25eV$.

352 Future rocket missions seeking to make high resolution measurements of photoelectrons
 353 should keep an eye out for this previously unreported spacecraft effect when the space-
 354 craft goes transonic.

355 **5.2 Refined Calculation of Ambipolar Field from Calibrated Data**

356 In this section we make three calculations of Earth’s ambipolar field: 1.) Above 620km
 357 where coulomb collisions are minimal, 2.) Below 530 km where there is no transonic cor-
 358 rection, and 3.) An average calculation over the entire flight to compare directly with
 359 the initial result by G. A. Collinson et al. (2024). In all cases we make a linear fit to the
 360 shift in PES data vs. altitude to determine the gradient, and hence calculate the par-
 361 allel electric field.

362 **5.2.1 Ambipolar field above 620km**

363 Above 620km the effect of coulomb collisions is predicted by STET to be very small, and
 364 thus PES data from these altitudes are ideal for searching for a clean measurement of
 365 Earth’s ambipolar field (which should be the dominant source of the energy shift in pho-
 366 toelectrons). Note that while this is only a fraction of the total altitude explored by *En-
 367 durance*, more than half of the PES measurements were collected above 620 km (from
 368 $\sim 01:36$ GMT to just after $\sim 01:42$ GMT, Fig. 1b), so there is ample data from this re-
 369 gion to analyze.

370 For the purposes of measuring a parallel electric field, all that is needed is the relative
 371 shift in photopeak energy (not the absolute shift). Analysis on data above 620km would
 372 yield the same result with or without the transonic calibration, since in this region the
 373 only correction factor is a constant $-0.25eV$ energy offset, and the gradient of the mea-
 374 sured energy shift is unaffected. We find that the relative shift in photopeaks measured
 375 by PES above 620 km closely matches theory (Fig. 2a data minus theory constant above
 376 620km), and thus is extremely consistent with what is expected for Earth’s ambipolar
 377 field. The total potential drop inferred from these measurements was ~ 0.23 , correspond-
 378 ing to a parallel electric field of $1.6\mu Vm^{-1}$ between 620km and 768 km.

379 **5.2.2 Ambipolar field below 530km**

380 Below 530km, data are unaffected by the transonic correction, and is thus another al-
 381 titude region where a clean measurement of Earth’s ambipolar field should be possible.
 382 In this region however, STET predicts that the total shift in photoelectrons ($\sim 0.22V$)
 383 is dominated by coulomb collisions. Taking the PES data, subtracting the shift at each
 384 altitude from STET, and applying a linear fit (not shown for brevity) yields a mean shift
 385 of $\sim 0.08eV$, corresponding to an electric field of $0.45\mu Vm^{-1}$ between 250km and 530km.
 386 This weaker electric field at low altitude is consistent with the prediction by SLP (Fig.
 387 1d).

388 **5.2.3 Average field over the flight**

389 If we accept the entire corrected dataset shown in Fig. 2c, we can subtract the coulomb
 390 collision shift predicted by STET to estimate the contribution solely from the ambipo-
 391 lar field throughout the flight. Caution must be taken with this approach, as STET was
 392 also involved in the transonic calibration, making this analysis partially circular above
 393 530km. Nonetheless, with this caveat, subtracting STET’s predicted coulomb collision
 394 shift at each altitude and applying the same linear fit as G. A. Collinson et al. (2024)
 395 (not shown for brevity) yields an estimated potential drop of $\sim 0.49V$, corresponding
 396 to an electric field of $0.97\mu Vm^{-1}$. This average falls between the high-altitude and low-
 397 altitude only estimates presented above. This result is also consistent within errors with
 398 the original calculation by G. A. Collinson et al. (2024) and thus generally supports the
 399 conclusions presented there. A safe conclusion from this analysis of the entire corrected
 400 dataset is that the effect of coulomb collisions was indeed much smaller than predicted
 401 by the pre-flight GLOW simulations and remained within the uncertainties of the orig-
 402 inal measurement.

403 **5.3 Assessment of the energy shift from Coulomb Collisions**

404 Modeling the effects of coulomb collisions on photopeaks is notoriously difficult and re-
 405 quires a very careful approach (Khazanov, 2010). We find that for precision (sub-electronvolt)
 406 measurements, a fully kinetic model is needed to accurately determine the effect of coulomb
 407 collisions. Our post-flight prediction by the kinetic STET model ($-0.37eV$) is less than
 408 the pre-flight prediction by G. A. Collinson, Glocer, Pfaff, et al. (2022) ($\sim -1eV$) which
 409 used the GLOW two-stream model (which as per Solomon (2017) handles coulomb col-
 410 lisions using the analytical formulation of Swartz et al. (1971)). A key factor distinguish-
 411 ing these approaches is that STET includes the simultaneous treatment of pitch-angle
 412 scattering and energy loss. We posit that treating these two processes together may be
 413 important for accurately capturing the precise energy shift of photoelectrons from coulomb
 414 collisions. However, for most applications where sub-electronvolt resolution is not required,
 415 GLOW would still be a resonable approximation, giving an order of magnitude agree-
 416 ment to the coulomb collisional shift observed by *Endurance*.

417 During the flight of *Endurance*, the transonic energy shift (hitherto unknown) of $+0.25eV$
 418 was countering and masking much of the shift from coulomb collisions. The recalibrated

419 data were found to be consistent over the entire flight (250km to 768km) with a com-
 420 bination of the dominant shift from Earth’s Ambipolar field and the weaker shift from
 421 coulomb collisions of $-0.37eV$ predicted by STET. During conditions of solar maximum
 422 the effect of coulomb collisions could likely be stronger, but the measurements here were
 423 selected to occur at low solar activity to deliberately minimize this effect.

424 6 Open Research

425 *Endurance* data are available from the NASA Goddard Space Flight Center Space Physics
 426 Data Facility <https://cdaweb.gsfc.nasa.gov>, by selecting “Sounding Rockets” as the
 427 data source.

428 Acknowledgments

429 We thank and acknowledge the 100+ strong team of engineers, scientists, and techni-
 430 cians who made the *Endurance* mission a success. *Endurance* was funded through the
 431 National Aeronautics and Space Administration Heliophysics Technology and Instrument
 432 Development for Science grant 80NSSC19K1206. This study was funded by the upcom-
 433 ing *Resolute* mission, funded through NASA’s Heliophysics Low Cost Access to Space
 434 (H-LCAS) program. EISCAT support was supported through the National Environment
 435 Research Council Grant NE/RO17000X/1. We thank D. Kotov for the private correspon-
 436 dences which helped us better appreciate the historical context of these measurements.
 437 We thank A.P. Collinson for support and useful discussions when preparing this manuscript.

438 References

- 439 Cicerone, R. J., & Bowhill, S. A. (1970, January). Photoelectron Escape Fluxes Ob-
 440 tained by a Monte Carlo Technique. *Radio Science*, *5*(1), 49-53. doi: 10.1029/
 441 RS005i001p00049
- 442 Coates, A. J., Johnstone, A. D., Sojka, J. J., & Wrenn, G. L. (1985, Novem-
 443 ber). Ionospheric photoelectrons observed in the magnetosphere at dis-
 444 tances up to 7 earth radii. *Planet. Space. Sci.*, *33*, 1267-1275. doi:
 445 10.1016/0032-0633(85)90005-4
- 446 Coates, A. J., Wellbrock, A., Waite, J. H., & Jones, G. H. (2015, June). A new up-
 447 per limit to the field-aligned potential near Titan. *Geophys. Res. Lett.*, *42*(12),
 448 4676-4684. doi: 10.1002/2015GL064474
- 449 Collinson, G., Mitchell, D., Glocer, A., Grebowsky, J., Peterson, W. K., Connerney,
 450 J., ... Jakosky, B. (2015, November). Electric Mars: The first direct mea-
 451 surement of an upper limit for the Martian “polar wind” electric potential.
 452 *Geophys. Res. Lett.*, *42*, 9128-9134. doi: 10.1002/2015GL065084
- 453 Collinson, G. A., Chornay, D. J., Glocer, A., Paschalidis, N., & Zesta, E. (2018,
 454 November). A hybrid electrostatic retarding potential analyzer for the mea-
 455 surement of plasmas at extremely high energy resolution. *Review of Scientific*
 456 *Instruments*, *89*(11), 113306. doi: 10.1063/1.5048926
- 457 Collinson, G. A., Frahm, R., Glocer, A., Coates, A. J., Grebowsky, J. M., Barabash,
 458 S., ... Zhang, T. L. (2016, June). The electric wind of Venus: A global
 459 and persistent “polar wind”-like ambipolar electric field sufficient for
 460 the direct escape of heavy ionospheric ions. *Geophys. Res. Lett.* doi:
 461 10.1002/2016GL068327
- 462 Collinson, G. A., Frahm, R. A., Glocer, A., Daldorff, L., Thiemann, E., Kang, S.-B.,
 463 ... Zhang, T. (2023, September). A Survey of Strong Electric Potential Drops
 464 in the Ionosphere of Venus. *Geophys. Res. Lett.*, *50*(18), e2023GL104989. doi:
 465 10.1029/2023GL104989
- 466 Collinson, G. A., Glocer, A., Chornay, D., Michell, R., Pfaff, R., Cameron, T., ...
 467 Paschalidis, N. (2022, September). Rocket Measurements of Electron Energy

- 468 Spectra From Earth's Photoelectron Production Layer. *Geophys. Res. Lett.*,
 469 49(17), e98209. doi: 10.1029/2022GL098209
- 470 Collinson, G. A., Glocer, A., Pfaff, R., Barjatya, A., Bissett, S., Blix, K., ... Wilson,
 471 T. (2022, August). The Endurance Rocket Mission. *Space Sci. Rev.*, 218(5),
 472 39. doi: 10.1007/s11214-022-00908-0
- 473 Collinson, G. A., Glocer, A., Pfaff, R., Barjatya, A., Conway, R., Breneman, A., ...
 474 Team, T. E. M. (2024). Earth's ambipolar electrostatic field and its role in ion
 475 escape to space. *Nature*, 632(8027), 1025. Retrieved from [https://doi.org/
 476 10.1038/s41586-024-07480-3](https://doi.org/10.1038/s41586-024-07480-3) doi: 10.1038/s41586-024-07480-3
- 477 Doering, J. P., Peterson, W. K., Bostrom, C. O., & Potemra, T. A. (1976, March).
 478 High resolution daytime photoelectron energy spectra from AE-E. *Geophys.*
 479 *Res. Lett.*, 3, 129-131. doi: 10.1029/GL003i003p00129
- 480 Glocer, A., Khazanov, G., & Liemohn, M. (2017). Photoelectrons in the quiet polar
 481 wind. *Journal of Geophysical Research: Space Physics*, 122(6), 6708–6726.
- 482 Gombosi, T. I., & Rasmussen, C. E. (1991, May). Transport of gyration-dominated
 483 space plasmas of thermal origin. I - Generalized transport equations. *J. Geo-*
 484 *phys. Res.*, 96, 7759-7778. doi: 10.1029/91JA00012
- 485 Jasperse, J. R., & Smith, E. R. (1978, October). The photoelectron flux in the
 486 Earth's ionosphere at energies in the vicinity of photoionization peaks. *Geo-*
 487 *phys. Res. Lett.*, 5(10), 843-846. doi: 10.1029/GL005i010p00843
- 488 Khazanov, G. V. (2010). *Kinetic Theory of the Inner Magnetospheric Plasma*
 489 (Vol. 372). New York, NY: Springer Science & Business Media.
- 490 Khazanov, G. V., Glocer, A., & Himwich, E. W. (2014, January). Magnetosphere-
 491 ionosphere energy interchange in the electron diffuse aurora. *Journal of Geo-*
 492 *physical Research (Space Physics)*, 119, 171-184. doi: 10.1002/2013JA019325
- 493 Khazanov, G. V., Liemohn, M. W., & Moore, T. E. (1997). Photoelectron effects on
 494 the self-consistent potential in the collisionless polar wind. *Journal of Geophys-*
 495 *ical Research*, 102(A), 7509–7522.
- 496 Lee, J. S., Doering, J. P., Bostrom, C. O., & Potemra, T. A. (1978, July). Mea-
 497 surement of the daytime photoelectron energy distribution from AE-E
 498 with improved energy resolution. *Geophys. Res. Lett.*, 5(7), 581-583. doi:
 499 10.1029/GL005i007p00581
- 500 Lee, J. S., Doering, J. P., Potemra, T. A., & Brace, L. H. (1980a, October). Mea-
 501 surements of the ambient photoelectron spectrum from atmosphere explorer: I.
 502 AE-E measurements below 300 km during solar minimum conditions. *Planet.*
 503 *Space. Sci.*, 28(10), 947-971. doi: 10.1016/0032-0633(80)90058-6
- 504 Lee, J. S., Doering, J. P., Potemra, T. A., & Brace, L. H. (1980b, October). Mea-
 505 surements of the ambient photoelectron spectrum from atmosphere explorer:
 506 II. AE-E measurements from 300 to 1000 km during solar minimum conditions.
 507 *Planet. Space. Sci.*, 28(10), 973-996. doi: 10.1016/0032-0633(80)90059-8
- 508 Peterson, W. K., Doering, J. P., Potemra, T. A., McEntire, R. W., & Bostrom,
 509 C. O. (1977, March). Conjugate photoelectron fluxes observed on Atmosphere
 510 Explorer C. *Geophys. Res. Lett.*, 4, 109-112. doi: 10.1029/GL004i003p00109
- 511 Solomon, S. C. (2017, July). Global modeling of thermospheric airglow in the far ul-
 512 traviolet. *Journal of Geophysical Research (Space Physics)*, 122(7), 7834-7848.
 513 doi: 10.1002/2017JA024314
- 514 Spitzer, L. (1950). *Physics of ionized gases*. Interscience Publishers.
- 515 Swartz, W. E., Nisbet, J. S., & Green, A. E. S. (1971, December). Analytic expres-
 516 sion for the energy-transfer rate from photoelectrons to thermal-electrons. *J.*
 517 *Geophys. Res.*, 76(34), 8425-8426. doi: 10.1029/JA076i034p08425
- 518 Xu, S., Mitchell, D., McFadden, J., Collinson, G., Harada, Y., Lillis, R., ... Conner-
 519 ney, J. (2018). Field-aligned potentials at Mars from MAVEN observations.
 520 *Geophys. Res. Lett.*